

Available online at [www.sciencerepository.org](http://www.sciencerepository.org)

Science Repository



## Research Article

# Olfactory Stem Cells for the Treatment of Spinal Cord Injury: Isolation, Purification and Behaviour in a Plasma Clot Matrix

Markus Rövekamp<sup>1</sup>, Stefan Volkenstein<sup>2</sup>, Amir Minovi<sup>3</sup>, Aliana Neubaur<sup>1</sup>, Stefan Dazert<sup>2</sup>, Mirko Aach<sup>4</sup>, Thomas Armin Schildhauer<sup>1</sup>, Manfred Köller<sup>1</sup> and Christina Sengstock<sup>1\*</sup>

<sup>1</sup>Surgical Research, BG University Hospital Bergmannsheil, Ruhr University Bochum, Bochum, Germany

<sup>2</sup>Department of Otorhinolaryngology, Head and Neck Surgery, St. Elisabeth Hospital, Ruhr University Bochum, Bochum, Germany

<sup>3</sup>Head, Neck and Ear Surgery, St. Elisabeth Hospital Hohenlind, Werthmannstr, Germany

<sup>4</sup>Department of Spinal Cord Injuries, BG University Hospital Bergmannsheil, Ruhr University Bochum, Bochum, Germany

### ARTICLE INFO

#### Article history:

Received 17 June, 2020

Accepted 1 July, 2020

Published 29 July, 2020

#### Keywords:

Olfactory mucosa  
olfactory stem cells  
cell therapy  
plasma clot matrix  
autologous cell transplantation  
spinal cord injury

### ABSTRACT

Cell therapies represent promising strategies to improve neurological functions after spinal cord injury (SCI). Olfactory mucosa (OM) might be an attractive source of multipotent cells for neuroregeneration because olfactory stem cells (OSCs) are resident. The regenerative capacity of OSCs has been demonstrated in animal models and some clinical case reports. Up to now, there are no standard methods for purification, characterization, and delivery of OSCs to the injury site. However, purification and characterization of the grafted cells are prerequisites for clinical use to ensure maximum safety for the patients. In this study, we isolated and purified OSCs from human OM using the neurosphere assay. Subsequently, the cells were characterized, and the behavior of purified OSCs in a plasma clot was investigated. Our study demonstrated that isolated cells from OM form neurospheres, which cells are positive for CD105 (98%) and CD90 (99%) and negative for Epcam (<1%) and MUC5AC (<1%). Purified OSCs were positive for Nestin, CD44 as well as GFAP and showed a lack of CD34 and CD45 expression. OSCs differentiated into neuron-like cells expressing  $\beta$ -III tubulin. However, differentiation into adipocytes, chondrocytes or osteoblast could not be observed. In addition, OSCs stayed viable and were able to proliferate within the plasma clot. These results highlight OSC as a candidate for autologous transplantation in combination with the plasma clot as a cell carrier in SCI and neurodegenerative disease.

© 2020 Christina Sengstock. Hosting by Science Repository.

## Introduction

Spinal cord injury (SCI) is one of the most devastating damages to the vertebral column. The majority of all injuries are traumatic due to physical impacts such as work-related injuries, sports, motor vehicle crashes and violence [1]. There are about 180.000 new SCI cases reported each year worldwide [2]. SCI results in mechanical damage of neuronal and glial cells, induction of pro-apoptotic signaling, ionic dysregulation and disruption of the microvasculature [3, 4]. The severity and location of the lesion influence the clinical outcome and may include partial or complete loss of sensory and motor function below the injury.

Despite different therapeutic options, including the use of neuroprotective agents and neural reparative therapeutic strategies such as methylprednisolone, minocycline, riluzole, glibenclamide, cethrin, granulocyte colony-stimulating factor, hypothermia, and anti-Nogo-A antibody, the treatment of SCI is quite limited, and a complete recovery without neurological deficits is almost impossible [5, 6]. Cell-therapeutic approaches may represent a promising treatment strategy, assuming that transplanted cells can differentiate, regenerate damaged circuits, substitute lost parts of tissue and modify the microenvironment through paracrine factors, extracellular matrix deposition and immune modulation [4, 5].

\*Correspondence to: Prof. Christina Sengstock, Bürkle-de-la-Camp-Platz 1, 44789 Bochum, Deutschland, Germany; Tel: +492343024724; E-mail: [christina.sengstock@rub.de](mailto:christina.sengstock@rub.de)

So far, different cells types have been used for the treatment of SCI including Schwann cells, embryonic stem cells, neuronal and mesenchymal stem cells (MSCs), induced pluripotent stem cells (iPSCs), as well as OSCs and olfactory ensheathing cells (OECs) [7-10]. Extraction of neural stem cells for autologous transplantation is challenging; however, there are only two neurogenic areas within the adult mammalian central nervous system where stem cells are resident: the olfactory bulb (OB) and the dentate gyrus of the hippocampus [11]. Since those areas are deep within the central nervous system (CNS), the risks of violation occur during extraction. The olfactory mucosa (OM) represents an optimal source for the isolation of autologous neural stem cells because the OM is located in the nasal cavity, is easily accessible and can be removed without loss of the olfactory sense. In general, olfactory tissue derives from the neural crest and remains in a stage of embryo-like development [12]. Neurogenic and neuroregenerative properties of the OM are attributed to both the OSCs and OECs [13]. The use of olfactory cells may be a promising treatment strategy for immunomodulation and tropic support after SCI, because OSCs (located in the epithelium layer) are able to proliferate and differentiate into receptor neurons and secrete a broad range of neurotrophic factors including glial cell-derived neurotrophic factor (GDNF), brain-derived neurotrophic factor (BDNF), nerve growth factor (NGF), Neurotrophin-3, NT-4 and vascular endothelial growth factor (VEGF) [14, 15].

In contrast to human embryonic stem cells or iPSCs the olfactory mucosa cells do not face ethical or technical issues [16]. Numerous preclinical studies, and some clinical trials used olfactory cells for repair of spinal cord injuries [17-21]. The safety and the feasibility of olfactory cell transplants were firstly demonstrated in the study of Lima, where 7 patients with ASIA class A received olfactory mucosa autografts [22]. All patients showed improvement in ASIA scores, two patients improved to ASIA C, and moderate to complete filling of the lesions site was observed [22]. However, as was shown in one case report by Dlouhy *et al.* complications occurred due to the co-transplantation of mucus-producing cells after total olfactory mucosal tissue transplantation [22, 23]. Thus, for safety reasons, it is important to establish standardized isolation and purification methods and to characterize the isolated cell fractions correctly to avoid unintended cell reactions [24].

Effects of cell therapies are dependent on the used cell type, the cell differentiation status, timing of delivery and the route of administration (intravenous, intrathecal, direct intramedullary injection or biomaterial-based application) [25]. Transplanted cells are not expected to survive at a high rate if injected directly and may not persist at the application site [26]. Thus, the deposition of cells requires a carrier or scaffold to avoid cell dispersion and to allow the capacity of the transplant to fill defect zones [27, 28]. In general, the uses of biomaterials may enhance the neuronal regeneration after SCI by acting as a structural guidance scaffold for the delivery of drugs or bioactive factors, supporting survival and differentiation of transplanted cells [4]. The autologous plasma clot might be a promising cell carrier due to excellent biocompatibility, biodegradability and three-dimensional structure, which allows storage and diffusion of bioactive factors [29-33]. As we have shown previously, a longitudinal alignment of fibrin fibers within a plasma clot can be achieved [34]. In addition, human plasma represents a favorable environment for cell therapeutic approaches due to the presence of growth factors, such as epithelial growth factor (EGF),

fibroblast growth factor (FGF), insulin-like growth factor-1 (IGF-1) and VEGF which promotes axonal regeneration [35].

Thus, the aim of this study was to develop a purification method for OSCs from the OM and to characterize the cells after cell isolation. In addition, the behavior of the purified OSCs from OM in a plasma clot matrix as a possible cell carrier for cell therapeutic approaches was studied.

## Materials and Methods

### I Mucosal Biopsies

Human biopsies from nasal mucosa were collected dorso-posterior from the top of the middle nasal turbinate from six volunteers by nasal endoscopy at the Department of Otorhinolaryngology, Head- and Neck Surgery/St. Elisabeth-Hospital Bochum. Sample acquisition was approved by the ethics committee of the Faculty of Medicine of the Ruhr University Bochum (16-5753-3-BR). The biopsies were immediately transferred into Dulbecco's Modified Eagle Media (DMEM)/F-12 Glutamax (Invitrogen GmbH, Karlsruhe, Germany) supplemented with 10% fetal calf serum (FCS, Sigma-Aldrich, Taufkirchen, Germany) containing antibiotic antimycotic solution (AAS, Sigma-Aldrich) and transported on ice to the cell culture lab.

### II Isolation and Purification of OSC

To separate the epithelium layer (ET) and the lamina propria (LP) from the OM the biopsies were washed three to five times with Hank's buffered salt solution (HBSS, Sigma-Aldrich) and incubated for 45 min in Dispase II solution (2.4 units ml<sup>-1</sup>; Sigma-Aldrich) at 37°C under cell culture conditions. The enzymatic reaction was stopped by adding DMEM/ F-12 Glutamax/ 10% FCS, followed by mechanical separation of the LP from the ET using a stereomicroscope and spring steel forceps.

To isolate the OSCs from the ET, the tissue was mechanically dissociated by gentle trituration using a micropipette until a homogenous cell suspension was obtained. Then the suspension was transferred to a 24-well plate (Falcon, BD Bioscience, Heidelberg, Germany) that had been pre-coated with poly-L-lysine (PLL; 50 µg cm<sup>-2</sup>; Sigma-Aldrich) overnight at 7°C. Incubation followed in DMEM/F-12 Glutamax/10% FCS/AAS under cell culture conditions for 14 days with a medium exchange every two or three days. Subsequently, the adherent cells were detached by 0.25% trypsin/0.05% ethylenediaminetetraacetic acid (v/v) (EDTA, Sigma-Aldrich) and transferred to cell culture flasks (75 cm<sup>-2</sup>, Falcon).

To purify OSCs from the epithelium layer, a neurosphere forming assay was used. In general, neurospheres represent clusters of neuronal differentiated and non-differentiated precursors and stem cells [36]. To generate neurospheres, 1×10<sup>5</sup> cells ml<sup>-1</sup> were seeded on PLL coated plates (Sarstedt, Nümbrecht, Germany) that had been pre-coated with poly-L-lysine (PLL; 100 µg cm<sup>-2</sup>; Sigma-Aldrich) overnight at 7°C in serum-free DMEM/F-12 Glutamax culture medium supplemented with insulin, transferrin, selenium (1% ITS, Sigma-Aldrich), 0.5 unit mL<sup>-1</sup> heparin (Sigma-Aldrich), 50 ng mL<sup>-1</sup> Fibroblast Growth Factor (FGF, Invitrogen) and 50 ng mL<sup>-1</sup> EGF (Epidermal Growth Factor, Invitrogen). After 3 days of incubation, cell cluster formation was visualized using

confocal laser scanning microscopy (CLSM, see below). After 5 days of incubation, formed neurospheres detached from the surface and were harvested, centrifuged at 1100g for 5 minutes and dispersed to single cells using a micropipette. Subsequently, the cells were seeded on 24-well plates (Falcon) in DMEM/F12-Glutamax/10% FCS/AAS with a medium change every 2-3 days to expand the cells.

### III Confocal Laser Scanning Microscopy

The expression of surface markers, such as MUC5AC (mucus-producing cells; anti-human MUC5AC AF555; Abcam, Cambridge, UK), Epcam (epithelial cells; anti-human EpCAM AF488, BioLegend, Koblenz, Germany), Nestin (Alexa Fluor® 647 Mouse Anti-Nestin, BD Bioscience) and CD90 (anti-human CD90 AF488; R&D Systems, Minneapolis, USA) was analysed by confocal laser scanning microscopy (CLSM; LSM 700, Carl Zeiss, Jena, Germany). For CLSM analysis, isolated cells before and cells after neurosphere assay were seeded on 4-well chamber slides ( $1 \times 10^5$  cell/ well, Sarstedt) and incubated overnight under cell culture conditions. Then, adherent cells were fixed and permeabilized with BD Cytotfixbuffer and BD Perm & Wash solution (BD Bioscience) according to the manufacturer's instructions. Subsequently, the cells were washed with phosphate-buffered saline solution (PBS; Gibco) and incubated with PBS/3% FCS for 30 minutes at RT to block unspecific epitopes. After washing with PBS, incubation with antibodies ( $10 \mu\text{g mL}^{-1}$  in PBS/3% FCS, BD Bioscience) was carried out according to the manufacturer's instructions followed by nuclei staining using Hoechst 33342 (Life-Technologies, Darmstadt, Germany). Finally, the cells were washed again with PBS, covered with PBS, and analysed microscopically (Zeiss LSM 700) before and after the neurosphere assay.

### IV Flow Cytometry

After OSCs purification by neurosphere assay the expression of CD34 (PE Mouse Anti-Human CD34; BD Bioscience), CD44 (FITC Mouse Anti-Human CD44; BD Bioscience), CD45 (FITC Mouse Anti-Human CD45; BD Bioscience), CD105 (anti-human CD105 FITC, BD Bioscience), CD90 (anti-human CD90 PE; BD Bioscience), Epcam (anti-human EpCAM FITC, BD Bioscience), Nestin (Alexa Fluor® 647 Mouse Anti-Nestin, BD Bioscience) and GFAP (Alexa Fluor® 647 Mouse anti-GFAP) was analysed using flow cytometry. Therefore, cells ( $1 \times 10^5$  cells / FACS tube) were fixed and permeabilized with BD Cytotfixbuffer and BD Perm & Wash solution according to the manufacturer's instructions. Fc-receptor binding was inhibited by FcR-blocking reagent (BD Bioscience). Subsequently, antibodies were added and incubated for 30 minutes at RT. Then, cells were washed and resuspended in  $500 \mu\text{l}$  DMEM /F-12 Glutamax/10% FCS/AAS and analysed by flow-cytometric measurement (FACSCalibur™, BD Bioscience, Heidelberg, Germany). Results were quantified using CellQuest TMI.2.2 software (BD Bioscience).

### V Human Mesenchymal Stem Cells in Cell Culture

Bone marrow derived human mesenchymal stem cells (BM-hMSCs; 5<sup>th</sup> to 10<sup>th</sup> passage, Lonza, Basel, Switzerland) served as control and were cultivated in cell culture medium RPMI1640 (GIBCO, Invitrogen) containing 10% (v/v) fetal calf serum (FCS; GIBCO, Invitrogen) and L-glutamine ( $0.3 \text{ g L}^{-1}$ ; GIBCO, Invitrogen) using  $75 \text{ cm}^2$  culture flasks

(BD Falcon). Cells were grown at  $37^\circ\text{C}$  in a humidified 5%  $\text{CO}_2$  atmosphere and sub-cultivated every 7 to 14 d depending on cell proliferation. After washing with PBS, growing hMSC were detached from the culture flasks by addition of  $0.2 \text{ mL cm}^{-2}$  0.25% trypsin/0.05% EDTA for 5 min at  $37^\circ\text{C}$ . Subsequently, cells were harvested, washed twice with RPMI/FCS and seeded at a density of  $1.5 \times 10^4$  cells per well in 24-well cell culture plates (BD Falcon).

### VI Cell Differentiation

To analyze the osteogenic, adipogenic and chondrogenic differentiation potential, purified OSCs were seeded into 24-well tissue culture plates (Falcon). After 24 h of incubation, the non-adherent cells were removed, and the adherent cells were washed and incubated with osteogenic, adipogenic or chondrogenic differentiation medium (Gibco) for 14 days. BM-hMSCs were used as a positive control due to their typical capacity to differentiate into osteoblasts, adipocytes and chondrocytes within respective differentiation media. Alizarin Red S staining (Sigma-Aldrich) was used to monitor the degree of mineralization of osteogenic differentiated cells. Briefly, cells were washed with PBS and fixed with 10% formaldehyde (Sigma-Aldrich) for 30 min. After fixation, the cells were washed three times with distilled water and stained with 1% Alizarin Red S solution for 5 min. Differentiation was monitored by EVOS xl core light microscope (PEQLAB Biotechnologie GMBH, Erlangen, Germany). Adipogenic differentiation of the cells was determined by staining intra-cytoplasmic lipids and lipoproteins in the vacuoles of cells using Bodipy<sup>493/503</sup> (Invitrogen). Briefly, after 14 d of incubation, the cells were washed twice with PBS, fixed with 10% formaldehyde for 10 min, and then stained with Bodipy<sup>493/503</sup> for 15 min. Subsequently, cells were washed twice with distilled water, and adipogenic differentiation was determined by fluorescence microscopy (Olympus BX61, Olympus, Hamburg, Germany).

To support chondrogenic differentiation, 400,000 cells were pelleted and incubated for 3 h under cell culture conditions. After cultivation, the prewarmed chondrogenic differentiation medium was added. After 21 d of cultivation, chondrogenic differentiation of the cells was determined depending on the synthesis of proteoglycans by chondrocytes via alcian blue staining. Briefly, cells were washed with PBS and fixed with 4% formaldehyde for 30 min. After fixation, the cells were washed three times with PBS and then stained with 1% alcian blue (in 0,1 N HCL) for 30 min. After washing three times with distilled water the neutralize the acidity, chondrogenic differentiation was determined by a light microscope.

To study the neuronal differentiation potential,  $1 \times 10^5$  cells were seeded on 4-well glass chamber slides (Falcon). After 24 hours of incubation, the medium was removed and 1 ml of a neuronal differentiation medium (Neurogenic Supplement 1:10 in Neurobasal Medium, PromoCell GmbH, Heidelberg, Germany) was added to the cells. Every 3 days, the differentiation medium was changed. After 10 days to detect neuronal differentiation, cells were stained by using  $\beta$ -III tubulin (Alexa Fluor 488 anti- $\beta$ -tubulin III, BD Bioscience) followed by cell nuclei staining using Hoechst33342 in PBS for 5 min incubation at RT. Finally, the cells were washed with PBS, and analysed by CLSM (Zeiss LSM 700 microscope).

## VII Behavior of Cells in a Plasma Clot Matrix

Peripheral blood (9 ml Monovette®, sodium citrate, Sarstedt AG & Co.) were obtained from healthy volunteers (approval #16-5753-5-BR, Ethics Committee of the Faculty of Medicine of the Ruhr University Bochum). Blood plasma was prepared by centrifugation (3000g, 45min, RT) to obtain cell-free plasma. After centrifugation, the blood was separated into two layers, and the resultant top layer was used as cell-free plasma for the experiments. For plasma clot preparation, isolated OSCs were adjusted to  $1 \times 10^4$  cells/ 250  $\mu$ L cell culture medium (in DMEM / F-12 Glutamax / 10% FCS) and mixed with 250  $\mu$ L plasma. Subsequently, 12.5  $\mu$ L calcium chloride (10% solution, Sigma-Aldrich) and 5  $\mu$ L fluorescence-labeled fibrinogen (1% solution, Alexa Flour 595, Invitrogen) were added. This combination of cells and plasma were immediately mixed and seeded to a 4-chamber chamber slide (Sarstedt). Plasma clotting proceeded in an incubator (Heraeus Instruments, Hanau, Germany) for 60 min at 37°C. After coagulation, the clots were covered with DMEM/F-12 Glutamax/10% FCS and incubated for different periods under cell culture conditions (24 hours, 72 hours and 5 days).

Finally, vital cells were stained with SYTO 9 Green Fluorescent Nucleic Acid Stain (Invitrogen) and analysed by CLSM. For analysis of the three-dimensional orientation of cells within the clot, z-stack images were taken with different angles. Using the software "ZEISS ZEN" slices of the clot were recorded every 8  $\mu$ m.

## Results

### I Purification of Olfactory Stem Cells by Neurosphere Assay

To purify OSCs from isolated OM cell fractions, the neurosphere assay was performed using PLL-coated plates and neurosphere-forming medium (DMEM, 50ng mL<sup>-1</sup> EGF; 50ng mL<sup>-1</sup> FGF and 1% ITS). Neurospheres represent cell clusters consisting of neuronal differentiated and non-differentiated precursor/stem cells. Figure 1 represents light- (Figures 1A-1C) and fluorescence microscopic images (Figure 1D) of neurospheres formed 3 days after cultivation in the neurosphere medium (Figure 1A white arrow). Neurospheres were harvested after 5 days in culture after cell detachment (Figure 1B).

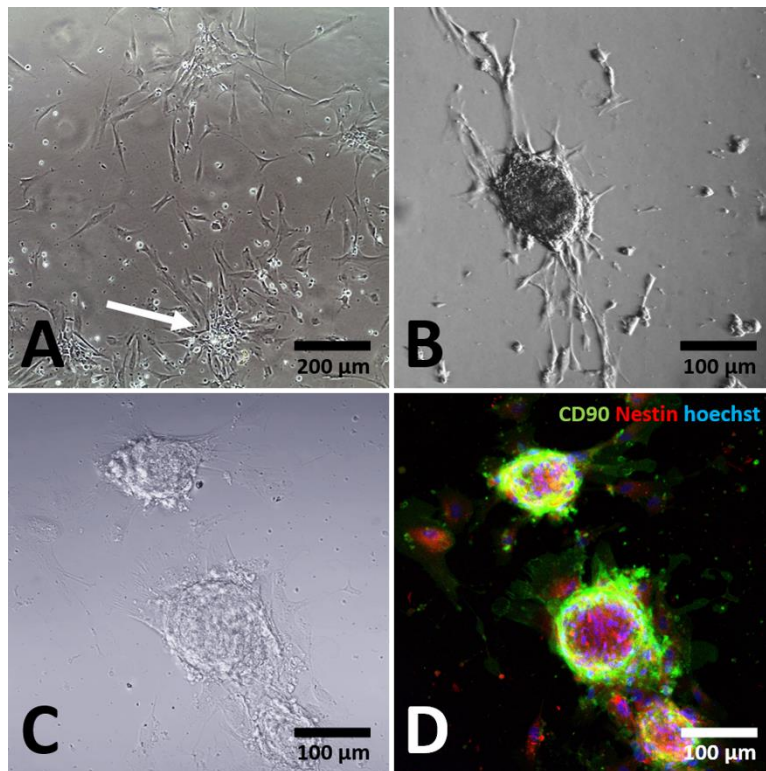


**Figure 1:** Light (A-C) and fluorescence (D) microscopic images of neurospheres formed after cultivation of an olfactory cell fraction in neurosphere-forming medium.

Isolated and passaged cells were cultivated in neurosphere-forming medium for 3 days (A) and 5 days (B). After 3 days in culture cells begin to form neurospheres (A, white arrow) which become detached and were harvested after 5 days (B & C). The neurospheres were positive for CD90 (green) and Nestin (red; D).

To characterize the cells, neurospheres were stained by CD90 (green fluorescence), Nestin (red fluorescence) and Hoechst 33342. OSC formed neurospheres (Figures 1A & 1C) which were harvested 5 days after detachment from cell culture plates (Figure 1B) and were positive for the neuronal marker Nestin and the mesenchymal cell surface marker CD90 (Figure 1D).

### II Immunohistochemical Characterization of Purified Olfactory Cells

To determine the purity of olfactory cells after neurosphere assay, immunohistochemical staining was used. Surface markers such as the cell surface marker CD90 (expressed on stem cells), the epithelial cell marker Epcam and MUC5AC to identify mucus-producing cells were



used. Cell nuclei were stained with Hoechst 33342. Human mesenchymal stem cells from bone marrow (BM-hMSCs) were used as control cells (Figures 2A & 2D). To determine whether mucus-producing cells and epithelial cells can be eliminated, isolated cells from

the olfactory mucosa (seeded on 4-well-chamber slides) before (Figures 2B & 2E) and after neurosphere assay (Figures 2C & 2F) were stained by different cell markers.

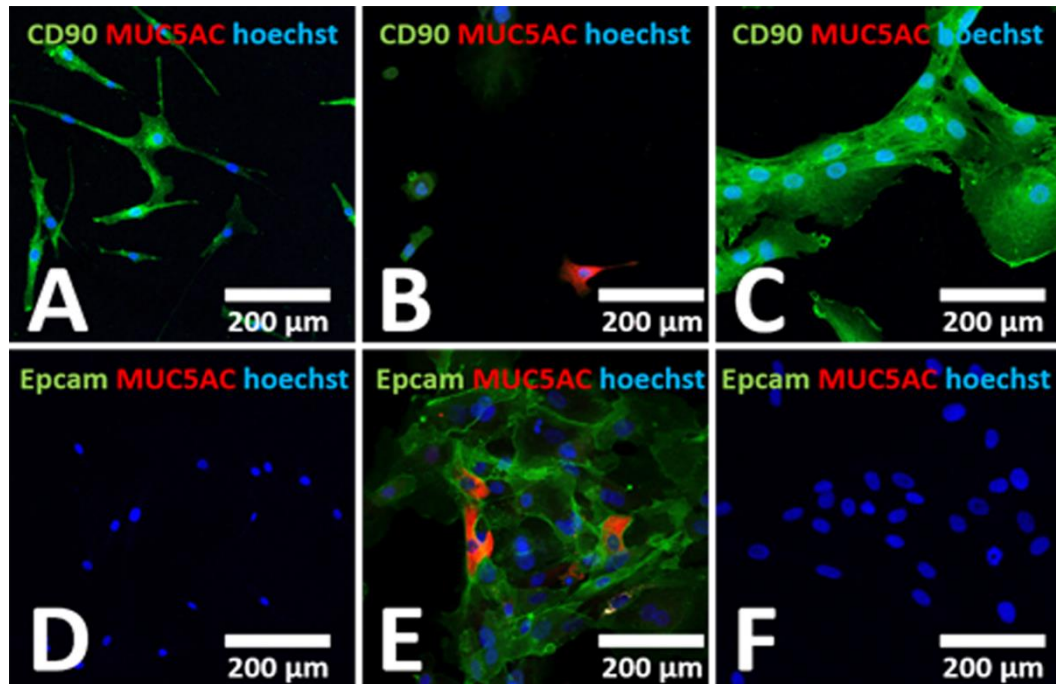


**Figure 2:** Confocal laser scanning microscopic images of isolated olfactory cells before and after neurosphere assay. Human BM-hMSCs were used as control (A & D). Cells were stained by using CD90 to identify stem cells, MUC5AC to identify mucus-producing cells and Epcam to visualize epithelial cells. Analyses were performed before (B & E) and after neurosphere assay (C & F). Cells isolated from OM were positive for CD90 similar to BM-hMSCs, and in addition to Epcam as well as MUC5A. After neurosphere formation Epcam and MUC5AC positive cells were eliminated in contrast to CD90 positive cells.

As shown in Figure 2, CD90 positive cells were found after isolation of the olfactory cell fraction (Figure 2B,  $78\% \pm 2$ ; analysed by flow cytometry) similar to BM-hMSCs (Figure 2A,  $98\% \pm 2$ ). These isolated cells from the ET of OM (before neurosphere assay) expressed the epithelial cell marker Epcam (Figure 2E,  $43\% \pm 28$ ) and single cells express MUC5AC (Figures 2B & 2E) in contrast to BM-hMSCs (Figures 2A & 2D). After the neurosphere assay of the OM cell fraction, CD90 positive cells were predominantly found (Figure 2C,  $99\% \pm 2$ ), and mucus-producing cells as well as epithelial cells, were not detectable (Figure 2F,  $<1\%$ ).

### III Flow Cytometric Characterization of Purified Olfactory Stem Cells

To further characterize purified OSCs, flow cytometry was used to determine the expression of neural differentiation markers such as Nestin, GFAP and CD44 and typical cell surface markers expressed on stem cells such as CD90 and CD105 as well as hematopoietic cell surface markers CD34 and CD45, which were not expressed on stem cells. In Figure 3, the histograms of the neuronal related markers Nestin (Figure 3A) and the glia/ neuronal cell marker CD44 (Figure 3B) as well as the astrocyte cell marker GFAP (Figure 3C) of the purified olfactory cell fraction are shown. In addition, the histograms of cell surface markers such as CD105 (Figure 3D), CD34 (Figure 3E), CD45 (Figure 3F) as well as CD90 (Figure 3G) and Epcam (Figure 3H) are represented. As

shown, olfactory neurosphere-forming cells expressed the markers GFAP, CD105, CD90, Nestin and CD44 in contrast to Epcam and hematopoietic cell surface markers such as CD34 and CD45 (Figure 3) which were not expressed.

### IV Differentiation Potential

To assess the tri-lineage differentiation of purified OSCs into mesodermal lineage (osteoblasts, adipocytes and chondrocytes) standard differentiation techniques were applied as reported previously [37]. To analyze the differentiation potential of OSCs into osteoblasts, Alizarin Red S staining was carried out to verify the mineralization of the cells. Purified OSCs showed no significant morphological changes or any osteogenic differentiation (Figure 4D) in contrast to bone marrow derived human mesenchymal stem cells in the presence of osteogenic differentiation media (Figure 4A).

To analyze adipogenic differentiation, lipid vesicles of the cells were visualized by Bodipy493/503 staining. As shown in Figure 4B, BM-hMSCs differentiated into adipocytes in the presence of adipogenic differentiation media (positive control; Figure 4B). The cells changed their morphology from a fibroblast-like form to a spherical one with intracellular lipid droplets (Figure 4B). In contrast to BM-hMSCs, purified OSCs (Figure 4E) do not form lipid droplets and adipogenic differentiation was not detectable (Figure 4E).

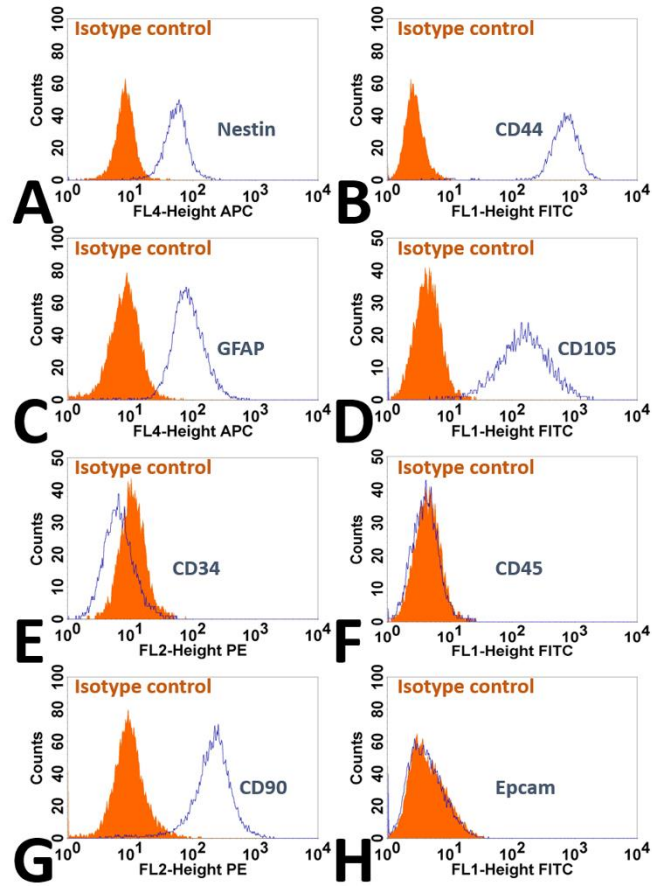


**Figure 3:** Flow cytometric overlay histograms of OSCs after purification.

**A)** Nestin (green), **B)** CD44 (blue curve), **C)** GFAP (green), **D)** CD105 (blue), **E)** CD34 (blue) and **F)** CD45 (blue), **G)** CD90 (blue), **H)** Epcam (blue). Isotype controls are orange histograms. Purified OSC are positive for Nestin, GFAP, CD105, CD90 as well as CD44 and negative for CD34, CD45 and Epcam.

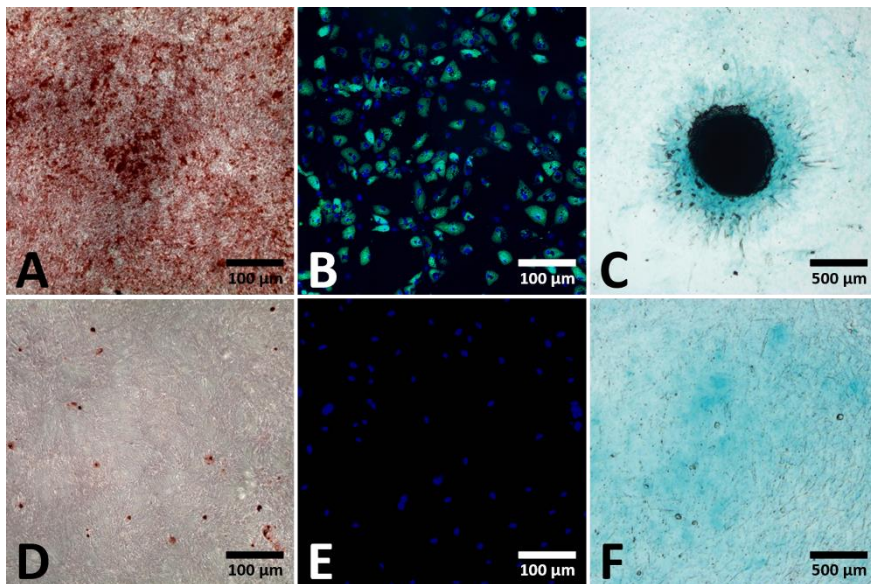


**Figure 4:** Differentiation capacity of human bone marrow mesenchymal stem cells (A-C) and OSCs (D-F). Light- (A, C, D & F) and fluorescence microscopic images (B & E) of BM-hMSCs (A-C) and OSCs (D-F) after cultivation in osteogenic (A & D), adipogenic (B & E) or chondrogenic differentiation medium (C & F) for 14-21 days. In contrast to BM-hMSCs (A-C) purified OSCs do not differentiate into osteogenic (B), adipogenic (E) or chondrogenic lineage (F).

Chondrogenic differentiation was analysed by alcian blue staining to visualize polyanionic glycosaminoglycan chains of proteoglycans in the cultured cells. In contrast to OSCs (Figure 4F), BM-hMSCs forming cartilage-like spheres in the presence of chondrogenic differentiation media (Figure 4C), which were alcian blue positive.

In order to detect the neuronal differentiation potential, OSCs were incubated in neuronal differentiation media for 7 days and the neuronal differentiation capacity was analysed by expression of  $\beta$ -III tubulin. BM-

hMSCs were used as control cells (Figures 5A & 5C). After cultivation in neuronal differentiation medium, OSCs obtained from OM (Figures 5B & 5D) changed their morphology to neuron-like cells as bipolar and multi-polarizing cells (white arrow, Figure 5B) in contrast to BM-hMSCs, which showed a fibroblast-like morphology (Figure 5A). Neuron-like cells from OM are positive for  $\beta$ -III tubulin (Figure 5D), while BM-hMSCs lack neuron-like morphology (Figure 5A) and expression of  $\beta$ -III tubulin (Figure 5C).

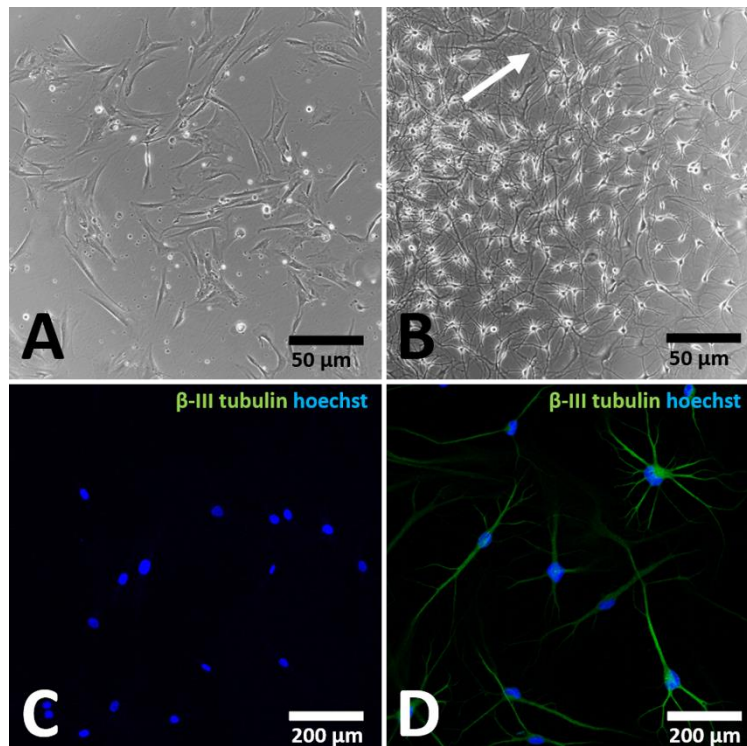


**Figure 5:** Neuronal differentiation capacity of BM-hMSCs and purified OSCs.

Light- (A & B) and fluorescence microscopic images (C & D) of OSC (B & D) and BM-hMSCs (A & C) after cultivation in neuronal differentiation medium for 7 days. In contrast to BM-hMSCs (A & C) which showed a fibroblast-like morphology (A), OSCs (B & D) showed a neuron-like morphology (B, white arrow) and were positive for  $\beta$ -III tubulin (D).

### V Cell Behavior in an Autologous Cell Carrier Matrix (Plasma Clot)

The delivery of cells to the defect site is still a clinical challenge. An autologous plasma clot matrix as a cell carrier could be used due to excellent biocompatibility and microporous three-dimensional structure, as we have shown previously [34]. Viability and proliferation of OSCs within such a cell carrier matrix was analysed by CLSM after different time points (24 hours, 3 days, 5 days). Figure 6 represents z-stack images of OSCs within the plasma clot after staining viable cells by SYTO 9 (green fluorescence) and fibrin fiber network by using Fibrinogen Alexa Fluor 594 (red fluorescence). As shown in Figure 6A, the front view image of the clot showed that viable OSCs are arranged three-dimensionally throughout the clot after 24h. Top view (Figure 6B) and side view (Figure 6C) images of the clot showed that the cells are well distributed, and morphology of the cells was similar to adherent cells in culture plates (Figure 1A). To analyze if cells can proliferate within a plasma clot matrix, OSCs and BM-hMSCs as control were incubated for 3 different time points (24 hours, 3 days, 5 days). Figure 7 represents

fluorescence images of cells after different time points within the matrix. SYTO 9 staining was performed to analyze whether cells are proliferating in the clot.

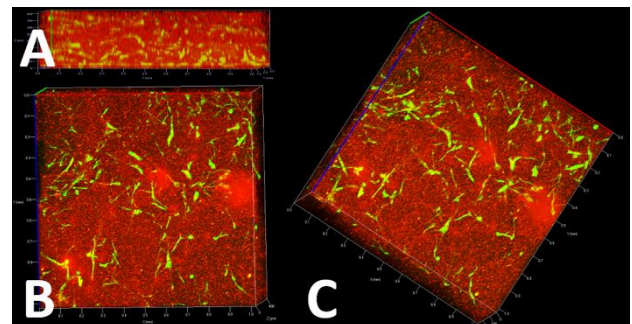


**Figure 6:** Fluorescence microscopic z-stack images of OSC within a plasma clot matrix. Viable cells were stained by using Syto 9 and fibrin fibers were stained by using Fibrinogen Alexa Fluor 594. A) front view; B) top view; C) side view. After 24h of incubation purified OSC stay viable within the plasma clot and arranged three-dimensional.



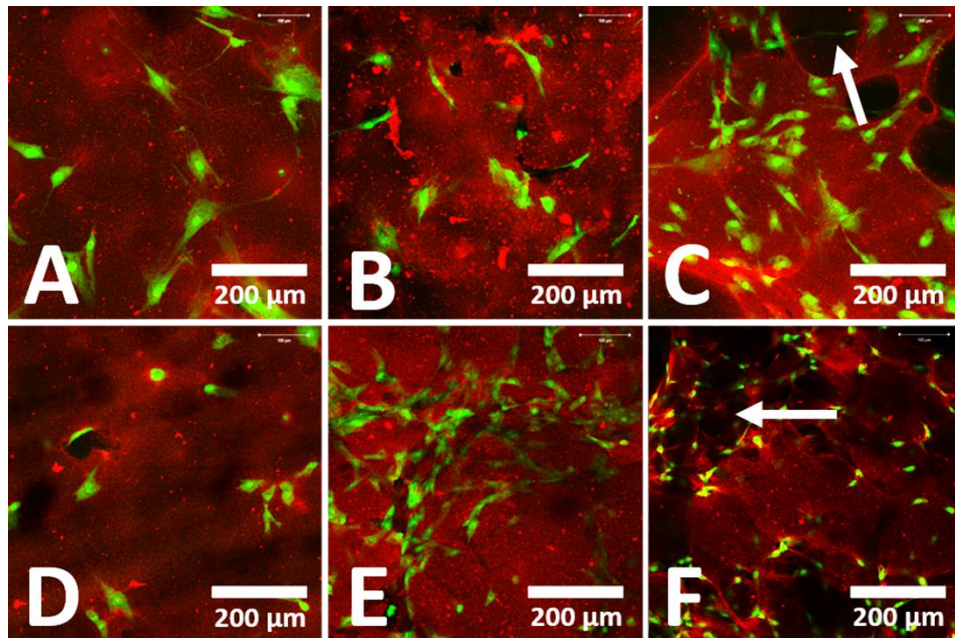


**Figure 7:** Cell behavior within a plasma clot matrix after different time points.

OSCs (**D-F**) and BM-hMSCs (**A-C**) after Syto-9 and Fibrinogen staining were performed to analyze whether cells are proliferating in the plasma clot matrix (**A & D**: 24h; **B & E**: 3 days and **C & F**: 5 days). After different time points purified OSCs (**D-F**) stay viable and proliferate within the matrix similar to BM-hMSCs (**A-C**), whereby the clot begin to degrade after 5 days in cell culture (**C & F**; white arrows).

As shown in (Figure 7), BM-hMSCs (Figures 7A, 7B & 7C) and OSCs (Figures 7D, 7E & 7F) were viable within the matrix and can proliferate after different time points. Cells were stained after 24 hours (Figures 7A & 7D), after 3 days (Figures 7B & 7E) and after 5 days (Figures 7C & 7F), whereby the clots begin to degrade (Figures 7F & 7C white arrows) due to physiological degradation which will occur faster with increasing cell number (data not shown).

## Discussion

A satisfying therapy for traumatic SCI remains still challenging, and therapeutic options to functionally restore a complete SCI are not available nowadays. Besides pharmaceutical treatment, physiotherapy, including locomotion therapy and movement stimulation systems, such as the Locomat or neurologic controlled exoskeletons like the Hybrid Assistive Limb Exoskeleton (HAL) are the golden standard [6, 38-41]. Cell therapies are only used experimentally [10]. Various cell therapies, such as the use of OSCs, have been tested in the last decade [19, 42-46]. Transplanted olfactory cells promoted tissue nerve regeneration by paracrine signaling and by creating a conducive environment [47]. Although these studies showed partial success, an insufficient cell purification can cause complications by co-transplantation of mucus-producing cells [22, 48, 49]. In addition, the injection of cells directly into the injury site can reduce the viability and functionality due to the inhibitory tissue environment [50]. Therefore, purification of transplanted OSCs to avoid possible unintended cell reactions after transplantation and an optimal cell carrier matrix to maintain the viability and functionality of the transplanted cells are necessary. The neurosphere assay, firstly reported by Reynolds and Weiss in 1992, is a well-described method to isolate and purify neuronal stem cells from different tissues [36]. We demonstrated that OSCs isolated from human OM formed neurospheres, which were positive for the neuronal marker

Nestin, an intermediate filament protein expressed in neural stem cells in the brain [51]. Mucus producing cells and epithelial cells were eliminated, in contrast to the purified CD90 and CD105 positive OSCs. These data are consistent with studies focusing on the behavior of human OSCs [52-54].

In addition to cell-surface characteristics, we analysed the differentiation potential of purified OSCs. In the presence of a neuronal differentiation medium, the cell morphology changes from a fibroblast-like morphology to an elongated, neuron-like morphology. Light microscopically bipolar and multipolar neuron-like cells could be observed, which were  $\beta$ -III tubulin positive. A comparable morphological change with  $\beta$ -III tubulin positive OSCs was demonstrated by Zhang *et al.* 2006 and others [53, 55-58]. As demonstrated by Murrell *et al.* and others, murine OSCs are neuronal precursor cells that have stem-cell-like abilities and are responsible for the renewal of the olfactory receptor neurons [59-62]. A study of Mackay-Sim 2010 showed similar data for cells isolated from the total OM. Since neurosphere formation, the expression of typical OSCs cell surface markers and neuronal differentiation are neuronal precursor cell characteristics, we confirmed that these purified cells in our study are neuronal precursor cells, the so-called OSCs [60-64].

In contrast to BM-hMSCs, purified OSCs could not be differentiated towards adipocytes, chondrocytes or osteoblasts. The literature about the differentiation potential of OSCs into mesodermal lineage is very inconsistent. While Leung *et al.* reported that differentiation of OSCs into mesenchymal cell types (adipocytes, chondrocytes or osteoblasts) could not be achieved, individual studies have shown that olfactory cells are also capable of forming non-neuronal cells [60-62]. It was demonstrated in a study of Ayala-Grosso *et al.* 2020, that olfactory cells isolated from the whole OM could differentiate into osteoblasts, adipocytes, chondroblasts and neuron-like cells, when cultured under



appropriate environment [65]. Interestingly, as reported by Delorme *et al.*, stem cells have also been found in the lamina propria of the OM, which are called ecto-mesenchymal stem cells due to their localization in the ectodermal tissue [66]. As reported in different studies, these ecto-mesenchymal stem cells, which express typical mesenchymal stem cell surface markers can differentiate into adipocytes, osteoblasts and chondrocytes [63, 67, 68]. In general, the ecto-mesenchymal stem cells have little in common with the neural olfactory stem cells, because according to Roisen *et al.*, these cells were able to form neurospheres and have mesenchymal characteristics but lack differentiation in neuron-like cells [53, 66]. Therefore, neuronal and mesodermal differentiation of cells from an entire OM can be explained by the presence of neuronal OSCs of the epithelial layer as well as ecto-mesenchymal stem cells of the lamina propria which are comparable in many respects with BM-hMSCs [65, 67]. Any adipogenic, chondrogenic or osteogenic differentiation of OSCs would not be desirable, especially when these cells were used for the treatment of SCI.

Besides the purity of transplanted cells, the surrounding signals in the local microenvironment will have an influence on SCI regeneration. After injection into the injury site, hostile local environment can reduce the viability and functionality of transplanted cells [50]. We agree with other groups suggesting using a cell carrier matrix to avoid immediate host rejection [26, 28]. In addition to hydrogels, silk fibroin biomaterials, chitosan-gelatin-agarose or poly-caprolactone, an autologous fibrin matrix is a good candidate for cell transplantations [34, 69-80]. In this study, we evaluated the loading of a plasma-clot matrix with the purified OSCs for future treatment of SCI. OSCs are viable within the plasma clot matrix and are able to proliferate after different time points. Furthermore, the clot dissolves after certain time due to physiological degradation of the plasma similar to the *in vivo* situation after implantation into injury site [81]. This degradation occurred faster with increasing cell numbers within the matrix. After clot degradation different growth factors like TNF- $\alpha$ , TGF- $\beta$ , PDGF, EGF or VEGF will be released and cell survival as well as cell proliferation is enhanced [82-84]. In general, the plasma clot represents a useful scaffold for transplantation due to many advantages and besides beneficial influence on OSCs, it can also be used as drug delivery system [85]. Furthermore, the fibrin clot structure can be modulated by numerous parameters such as calcium ions, pH, fibrinogen and thrombin. A fibrin clot, which is formed in the presence of a high thrombin concentration, consists of many thin fibrin fibers and smaller pores, whereas a low thrombin concentration results in the formation of thicker fibrin fibers and larger pores [86].

## Conclusion

In conclusion, different therapeutic interventions for patients suffering from SCI have shown promising results in preclinical or animal studies. However, in most of these studies SCI / neural recovery remains incomplete. Therefore, additional strategies such as stem cell-based options are necessary. Due to the inherent potential of OSCs for neurogenesis and the observed lower potential to differentiate into osteoblasts and adipocytes, OSCs are a promising candidate for cell therapy in traumatic spinal cord lesions. Previously described side effects, caused by simultaneously transplanted mucus producing cells, can be avoided by purification of OSCs using the neurosphere assay as demonstrated. In addition, for the first time in our knowledge, we have

shown that OSCs stay viable and can proliferate within a plasma-clot matrix as a potential cell carrier vehicle. In general, a combination of various treatment strategies addressing different aspects of SCI pathology would have greater beneficial outcomes. Here, the association of OSCs with an autologous plasma clot matrix may help to localize a targeted therapy of cell-based treatment in SCI. In summary, these results and previous studies highlight OSCs as candidate stem cells for autologous transplantation in SCI and neurodegenerative disease.

## Funding

This work was supported by a research grant from the German Statutory Accident Insurance (Deutsche Gesetzliche Unfallversicherung, DGUV).

## Competing Interests

None.

## REFERENCES

1. Ing Christine Höfer, Rolf Lefering (2018) TR-DGU\_annual\_report\_2018. *TraumaRegister DGU®*
2. B B Lee, R A Cripps, M Fitzharris, P C Wing (2014) The global map for traumatic spinal cord injury epidemiology: update 2011, global incidence rate. *Spinal Cord* 52: 110-116. [[Crossref](#)]
3. Hao Ren, Xuri Chen, Mengya Tian, Jing Zhou, Hongwei Ouyang et al. (2018) Regulation of Inflammatory Cytokines for Spinal Cord Injury Repair Through Local Delivery of Therapeutic Agents. *Advanced Science (Weinh)* 5: 1800529. [[Crossref](#)]
4. Jetan H Badhiwala, Christopher S Ahuja, Michael G Fehlings (2018) Time is spine. A review of translational advances in spinal cord injury. *J Neurosurg Spine* 30: 1-18. [[Crossref](#)]
5. Inês M Pereira, Ana Marote, António J Salgado, Nuno A Silva (2019) Filling the Gap: Neural Stem Cells as A Promising Therapy for Spinal Cord Injury. *Pharmaceuticals (Basel)* 12: 65. [[Crossref](#)]
6. Antígona Ulndreaj, Anna Badner, Michael G Fehlings (2017) Promising neuroprotective strategies for traumatic spinal cord injury with a focus on the differential effects among anatomical levels of injury. *F1000Res* 6: 1907. [[Crossref](#)]
7. Soraya Mehrabi, Sanaz Eftekhari, Fateme Moradi, Hamdollah Delaviz, Bagher Pourheidari et al. (2013) Cell therapy in spinal cord injury. A mini-review. *Basic Clin Neurosci* 4: 172-176. [[Crossref](#)]
8. Peggy Assinck, Greg J Duncan, Brett J Hilton, Jason R Plemel, Wolfram Tetzlaff (2017) Cell transplantation therapy for spinal cord injury. *Nat Neurosci* 20: 637-647. [[Crossref](#)]
9. Beatrice Sandner, Mareva Ciatipis, Melanie Motsch, Irina Soljanik, Norbert Weidner et al. (2016) Limited Functional Effects of Subacute Syngeneic Bone Marrow Stromal Cell Transplantation After Rat Spinal Cord Contusion Injury. *Cell Transplant* 25: 125-139. [[Crossref](#)]
10. Andrea J Mothe, Charles H Tator (2013) Review of transplantation of neural stem/progenitor cells for spinal cord injury. *Int J Dev Neurosci* 31: 701-713. [[Crossref](#)]
11. Rebecca M Ruddy, Cindi M Morshead (2018) Home sweet home. The neural stem cell niche throughout development and after injury. *Cell Tissue Res* 371: 125-141. [[Crossref](#)]
12. Audrey Chabrat, Emmanuelle Lacassagne, Rodolphe Billiras, Sophie Landron, Amélie Pontisso Mahout et al. (2019) Pharmacological

- Transdifferentiation of Human Nasal Olfactory Stem Cells into Dopaminergic Neurons. *Stem Cells Int* 2019; 2945435. [[Crossref](#)]
13. R J Franklin, S C Barnett (2000) Olfactory ensheathing cells and CNS regeneration. The sweet smell of success? *Neuron* 28: 15-18. [[Crossref](#)]
  14. Durai Murugan Muniswami, George Tharion (2018) Functional Recovery Following the Transplantation of Olfactory Ensheathing Cells in Rat Spinal Cord Injury Model. *Asian Spine J* 12: 998-1009. [[Crossref](#)]
  15. Irma Vismara, Simonetta Papa, Filippo Rossi, Gianluigi Forloni, Pietro Veglianesi (2017) Current Options for Cell Therapy in Spinal Cord Injury. *Trends Mol Med* 23: 831-849. [[Crossref](#)]
  16. Nancy Mp King, Jacob Perrin (2014) Ethical issues in stem cell research and therapy. *Stem Cell Res Ther* 5: 85. [[Crossref](#)]
  17. F Féron, C Perry, J Cochrane, P Licina, A Nowitzke et al. (2005) Autologous olfactory ensheathing cell transplantation in human spinal cord injury. *Brain* 128: 2951-2960. [[Crossref](#)]
  18. G Raisman (2001) Olfactory ensheathing cells - another miracle cure for spinal cord injury? *Nat Rev Neurosci* 2: 369-375. [[Crossref](#)]
  19. Susan L Lindsay, Andrew Toft, Jacob Griffin, Ahmed M M Emraja, Susan Carol Barnett et al. (2017) Human olfactory mesenchymal stromal cell transplants promote remyelination and earlier improvement in gait co-ordination after spinal cord injury. *Glia* 65: 639-656. [[Crossref](#)]
  20. Masahiro Ishihara, Noriko Mochizuki Oda, Koichi Iwatsuki, Haruhiko Kishima, Yu ichiro Ohnishi et al. (2014) Primary olfactory mucosal cells promote axonal outgrowth in a three-dimensional assay. *J Neurosci Res* 92: 847-855. [[Crossref](#)]
  21. Jian Gu, He Xu, Ya Ping Xu, Huan Hai Liu, Jun Tian Lang et al. (2019) Olfactory ensheathing cells promote nerve regeneration and functional recovery after facial nerve defects. *Neural Regen Res* 14: 124-131. [[Crossref](#)]
  22. Carlos Lima, José Pratas Vital, Pedro Escada, Armando Hasse Ferreira, Clara Capucho et al. (2006) Olfactory mucosa autografts in human spinal cord injury: a pilot clinical study. *J Spinal Cord Med* 29: 191-203. [[Crossref](#)]
  23. Brian J Dlouhy, Olatilewa Awe, Rajesh C Rao, Patricia A Kirby, Patrick W Hitchon (2014) Autograft-derived spinal cord mass following olfactory mucosal cell transplantation in a spinal cord injury patient: Case report. *J Neurosurg Spine* 21: 618-622. [[Crossref](#)]
  24. Peter J Andrews, Anne Lise Poirrier, Valerie J Lund, David Choi (2016) Safety of human olfactory mucosal biopsy for the purpose of olfactory ensheathing cell harvest and nerve repair. A prospective controlled study in patients undergoing endoscopic sinus surgery. *Rhinology* 54: 183-191. [[Crossref](#)]
  25. Serena Silvestro, Placido Bramanti, Oriana Trubiani, Emanuela Mazzon (2020) Stem Cells Therapy for Spinal Cord Injury: An Overview of Clinical Trials. *Int J Mol Sci* 21: 659. [[Crossref](#)]
  26. T A Schildhauer, D Seybold, J Geßmann, G Muhr, M Köller (2007) Fixation of porous calcium phosphate with expanded bone marrow cells using an autologous plasma clot. *Mat Wiss u. Werkstofftech* 38: 1012-1014.
  27. Wendy Ho, Bill Tawil, James C Y Dunn, Benjamin M Wu (2006) The behavior of human mesenchymal stem cells in 3D fibrin clots. Dependence on fibrinogen concentration and clot structure. *Tissue Eng* 12: 1587-1595. [[Crossref](#)]
  28. Shengwen Liu, Thomas Schackel, Norbert Weidner, Radhika Puttagunta (2017) Biomaterial-Supported Cell Transplantation Treatments for Spinal Cord Injury: Challenges and Perspectives. *Front Cell Neurosci* 11: 430. [[Crossref](#)]
  29. Beate Tschoeke, Thomas C Flanagan, Sabine Koch, Marvi Sri Harwoko, Thorsten Deichmann et al. (2009) Tissue-engineered small-caliber vascular graft based on a novel biodegradable composite fibrin-poly lactide scaffold. *Tissue Eng Part A* 15: 1909-1918. [[Crossref](#)]
  30. Mariève Talbot, Patrick Carrier, Claude J Giasson, Alexandre Deschambeault, Sylvain L Guérin et al. (2006) Autologous transplantation of rabbit limbal epithelia cultured on fibrin gels for ocular surface reconstruction. *Mol Vis* 12: 65-75. [[Crossref](#)]
  31. Anja M Boos, Annika Weigand, Gloria Deschler, Thomas Gerber, Andreas Arkudas et al. (2014) Autologous serum improves bone formation in a primary stable silica-embedded nanohydroxyapatite bone substitute in combination with mesenchymal stem cells and rhBMP-2 in the sheep model. *Int J Nanomedicine* 9: 5317-5339. [[Crossref](#)]
  32. Frank L Acosta Jr, Lionel Metz, Huston Davis Adkisson, Jane Liu, Ellen Carruthers Liebenberg et al. (2011) Porcine intervertebral disc repair using allogeneic juvenile articular chondrocytes or mesenchymal stem cells. *Tissue Eng Part A* 17: 3045-3055. [[Crossref](#)]
  33. Robert A Campbell, Maria Aleman, Laura D Gray, Michael R Falvo, Alisa S Wolberg (2010) Flow profoundly influences fibrin network structure: implications for fibrin formation and clot stability in haemostasis. *Thromb Haemostasis* 104: 1281-1284. [[Crossref](#)]
  34. Jan Gessmann, Dominik Seybold, Elvira Peter, Thomas Armin Schildhauer, Manfred Köller (2016) Alignment of the Fibrin Network Within an Autologous Plasma Clot. *Tissue Eng Part C Methods* 22: 30-37. [[Crossref](#)]
  35. Nan Fu Chen, Chun Sung Sung, Zhi Hong Wen, Chun Hong Chen, Chien Wei Feng et al. (2018) Therapeutic Effect of Platelet-Rich Plasma in Rat Spinal Cord Injuries. *Front Neurosci* 12: 252. [[Crossref](#)]
  36. Loic P Deleyrolle, Brent A Reynolds (2009) Isolation, expansion, and differentiation of adult Mammalian neural stem and progenitor cells using the neurosphere assay. *Methods Mol Biol* 549: 91-101. [[Crossref](#)]
  37. Le B Hang Pham, Yie Ri Yoo, Sun Hwa Park, Sang A Back, Sung Won Kim et al. (2017) Investigating the effect of fibulin-1 on the differentiation of human nasal inferior turbinate-derived mesenchymal stem cells into osteoblasts. *J Biomed Mater Res A* 105: 2291-2298. [[Crossref](#)]
  38. Shushi Kabu, Yue Gao, Brian K Kwon, Vinod Labhasetwar (2015) Drug delivery, cell-based therapies, and tissue engineering approaches for spinal cord injury. *J Control* 219: 141-154. [[Crossref](#)]
  39. M Aach, R C Meindl, J Geßmann, T A Schildhauer, M. Citak et al. (2015) Exoskelette in der Rehabilitation Querschnittgelähmter. Möglichkeiten und Grenzen. *Der Unfallchirurg* 118: 130-137.
  40. L Lünenburger, Gery Colombo, Robert Riener, Volker Dietz (2004) Biofeedback in gait training with the robotic orthosis Lokomat. *Conf Proc IEEE Eng Med Biol Soc* 2004: 4888-4891. [[Crossref](#)]
  41. J Mehrholz, L A Harvey, S Thomas, B Elsner (2017) Is body-weight-supported treadmill training or robotic-assisted gait training superior to overground gait training and other forms of physiotherapy in people with spinal cord injury? A systematic review. *Spinal Cord* 55: 722-729. [[Crossref](#)]
  42. Vijay G Goni, Rajesh Chhabra, Ashok Gupta, Neelam Marwaha, Mandeep S Dhillon et al. (2014) Safety profile, feasibility and early clinical outcome of cotransplantation of olfactory mucosa and bone marrow stem cells in chronic spinal cord injury patients. *Asian Spine J* 8: 484-490. [[Crossref](#)]

43. Pawel Tabakow, Wlodzimierz Jarmundowicz, Bogdan Czapiga, Wojciech Fortuna, Ryszard Miedzybrodzki et al. (2013) Transplantation of autologous olfactory ensheathing cells in complete human spinal cord injury. *Cell Transplant* 22: 1591-1612. [[Crossref](#)]
44. Pawel Tabakow, Geoffrey Raisman, Wojciech Fortuna, Marcin Czyz, Juliusz Huber et al. (2014) Functional regeneration of supraspinal connections in a patient with transected spinal cord following transplantation of bulbar olfactory ensheathing cells with peripheral nerve bridging. *Cell Transplant* 23: 1631-1655. [[Crossref](#)]
45. Yaojian Rao, Wenxiao Zhu, Yanxing Guo, Chunxia Jia, Ran Qi et al. (2013) Long-term outcome of olfactory ensheathing cell transplantation in six patients with chronic complete spinal cord injury. *Cell Transplant* 22 Suppl 1: S21-S25. [[Crossref](#)]
46. Yaojian Rao, Wenxiao Zhu, Huijuan Liu, Chunxia Jia, Qingan Zhao et al. (2013) Clinical application of olfactory ensheathing cells in the treatment of spinal cord injury. *J Int Med Res* 41: 473-481. [[Crossref](#)]
47. Krzysztof Marycz, Dariusz Szarek, Jakub Grzesiak, Karol Wrzeszcz (2014) Influence of modified alginate hydrogels on mesenchymal stem cells and olfactory bulb-derived glial cells cultures. *Biomed Mater Eng* 24: 1625-1637. [[Crossref](#)]
48. Carlos Lima, Pedro Escada, José Pratas Vital, Catarina Branco, Carlo Alberto Arcangeli et al. (2010) Olfactory mucosal autografts and rehabilitation for chronic traumatic spinal cord injury. *Neurorehabil Neural Repair* 24: 10-22. [[Crossref](#)]
49. Shinichi Esaki, Sachiyo Katsumi, Yuki Hamajima, Yoshihisa Nakamura, Shingo Murakami (2019) Transplantation of Olfactory Stem Cells with Biodegradable Hydrogel Accelerates Facial Nerve Regeneration After Crush Injury. *Stem Cells Transl Med* 8: 169-178. [[Crossref](#)]
50. Laura M Marquardt, Sarah C Heilshorn (2016) Design of Injectable Materials to Improve Stem Cell Transplantation. *Curr Stem Cell Rep* 2: 207-220. [[Crossref](#)]
51. U Lendahl, L B Zimmerman, R D McKay (1990) CNS stem cells express a new class of intermediate filament protein. *Cell* 60: 585-595. [[Crossref](#)]
52. Andrew Wetzig, Ayodele Alaiya, Monther Al Alwan, Christian Benedict Pradez, Manogaran S Pulicat et al. (2013) Differential marker expression by cultures rich in mesenchymal stem cells. *BMC Cell Biol* 14: 54. [[Crossref](#)]
53. F J Roisen, K M Klueber, C L Lu, L M Hatcher, A Dozier et al. (2001) Adult human olfactory stem cells. *Brain Res* 890: 11-22. [[Crossref](#)]
54. Dylana Diaz Solano, Olga Wittig, Carlos Ayala Grosso, Rosalinda Pieruzzini, Jose E Cardier (2012) Human olfactory mucosa multipotent mesenchymal stromal cells promote survival, proliferation, and differentiation of human hematopoietic cells. *Stem Cells Dev* 21: 3187-3196. [[Crossref](#)]
55. Xiaodong Zhang, Kathleen M Klueber, Zhanfang Guo, Jun Cai, Chengliang Lu et al. (2006) Induction of neuronal differentiation of adult human olfactory neuroepithelial-derived progenitors. *Brain Res* 1073-1074:109-119. [[Crossref](#)]
56. Emmanuel Nivet, Michel Vignes, Stéphane D Girard, Caroline Pierrisnard, Nathalie Baril et al. (2011) Engraftment of human nasal olfactory stem cells restores neuroplasticity in mice with hippocampal lesions. *J Clin Invest* 121: 2808-2820. [[Crossref](#)]
57. Steven A Johnstone, Martha Liley, Matthew J Dalby, Susan C Barnett (2015) Comparison of human olfactory and skeletal MSCs using osteogenic nanotopography to demonstrate bone-specific bioactivity of the surfaces. *Acta Biomater* 13: 266-276. [[Crossref](#)]
58. Mark Jakob, Hatim Hemed, Sandra Janeschik, Friedrich Bootz, Nicole Rotter et al. (2010) Human nasal mucosa contains tissue-resident immunologically responsive mesenchymal stromal cells. *Stem Cells Dev* 19: 635-644. [[Crossref](#)]
59. Wayne Murrell, François Féron, Andrew Wetzig, Nick Cameron, Karisha Splatt et al. (2005) Multipotent stem cells from adult olfactory mucosa. *Dev Dyn* 233: 496-515. [[Crossref](#)]
60. Xueyan Chen, Hengsheng Fang, James E Schwob (2004) Multipotency of purified, transplanted globose basal cells in olfactory epithelium. *J Comp Neurol* 469: 457-474. [[Crossref](#)]
61. J M Huard, S L Youngentob, B J Goldstein, M B Luskin, J E Schwob (1998) Adult olfactory epithelium contains multipotent progenitors that give rise to neurons and non-neural cells. *J Comp Neurol* 400: 469-486. [[Crossref](#)]
62. Cheuk T Leung, Pierre A Coulombe, Randall R Reed (2007) Contribution of olfactory neural stem cells to tissue maintenance and regeneration. *Nat Neurosci* 10: 720-726. [[Crossref](#)]
63. Mercedes Tomé, Susan L Lindsay, John S Riddell, Susan C Barnett (2009) Identification of nonepithelial multipotent cells in the embryonic olfactory mucosa. *Stem Cells* 27: 2196-2208. [[Crossref](#)]
64. Josephine B Jensen, Malin Parmar (2006) Strengths and limitations of the neurosphere culture system. *Mol Neurobiol* 34: 153-161. [[Crossref](#)]
65. Carlos Ayala Grosso, Rosalinda Pieruzzini, Leslie Vargas Saturno, José E. Cardier (2020) Las células mesenquimales del estroma olfatorio humano coexpresan proteínas de las células basales horizontales y de recubrimiento neural en cultivo. *Biomedica* 40: 72-88.
66. Bruno Delorme, Emmanuel Nivet, Julien Gaillard, Thomas Häupl, Jochen Ringe et al. (2010) The human nose harbors a niche of olfactory ectomesenchymal stem cells displaying neurogenic and osteogenic properties. *Stem Cells Dev* 19: 853-866. [[Crossref](#)]
67. Susan L Lindsay, Steven A Johnstone, Joanne C Mountford, Saghir Sheikh, David B Allan et al. (2013) Human mesenchymal stem cells isolated from olfactory biopsies but not bone enhance CNS myelination in vitro. *Glia* 61: 368-382. [[Crossref](#)]
68. Ke Rui, Zhijiang Zhang, Jie Tian, Xiang Lin, Xiaohui Wang et al. (2016) Olfactory ecto-mesenchymal stem cells possess immunoregulatory function and suppress autoimmune arthritis. *Cellular Mol Immunol* 13: 401-408. [[Crossref](#)]
69. Aiswarya Viswanath, Julie Vanacker, Loïc Germain, Julian G Leprince, Anibal Diogenes et al. (2017) Extracellular matrix-derived hydrogels for dental stem cell delivery. *J Biomed Mater Research A* 105: 319-328. [[Crossref](#)]
70. Wei Fu, Peng Xu, Bei Feng, Yang Lu, Jie Bai et al. (2019) A hydrogel derived from acellular blood vessel extracellular matrix to promote angiogenesis. *J Biomater Appl* 33:1301-1313. [[Crossref](#)]
71. Vince Beachley, Garret Ma, Chris Papadimitriou, Matt Gibson, Michael Corvelli et al. (2018) Extracellular matrix particle-glycosaminoglycan composite hydrogels for regenerative medicine applications. *J Biomed Mater Res A* 106: 147-159. [[Crossref](#)]
72. Wei Zhang, Longkun Chen, Jialin Chen, Lingshuang Wang, Xuexian Gui et al. (2017) Silk Fibroin Biomaterial Shows Safe and Effective Wound Healing in Animal Models and a Randomized Controlled Clinical Trial. *Adv Healthc Mater* 6. [[Crossref](#)]
73. Lijuan Xu, Shufang Wang, Xiang Sui, Yu Wang, Yanan Su et al. (2017) Mesenchymal Stem Cell-Seeded Regenerated Silk Fibroin Complex Matrices for Liver Regeneration in an Animal Model of Acute Liver Failure. *ACS Appl Mater Interfaces* 9: 14716-14723. [[Crossref](#)]



74. M M Moisenovich, E Y Plotnikov, A M Moysenovich, D N Silachev, T I Danilina et al. (2018) Effect of Silk Fibroin on Neuroregeneration After Traumatic Brain Injury. *Neurochem Res* 44: 2261-2272. [[Crossref](#)]
75. Vicky J Nelson, M F K Dinnunhan, Paul R Turner, Jim M Faed, Jaydee D Cabral (2017) A chitosan/dextran-based hydrogel as a delivery vehicle of human bone-marrow derived mesenchymal stem cells. *Biomed Mater* 12: 35012. [[Crossref](#)]
76. Zohreh Bagher, Zhaleh Atoufi, Rafieh Alizadeh, Mohammad Farhadi, Payam Zarrintaj et al. (2019) Conductive hydrogel based on chitosan-aniline pentamer/gelatin/agarose significantly promoted motor neuron-like cells differentiation of human olfactory ecto-mesenchymal stem cells. *Mater Sci Eng C Mater Biol Appl* 101: 243-253. [[Crossref](#)]
77. Hongfan Sun, Lin Mei, Cunxian Song, Xiumin Cui, Pengyan Wang (2006) The in vivo degradation, absorption and excretion of PCL-based implant. *Biomaterials* 27: 1735-1740. [[Crossref](#)]
78. Jorge Más Estellés, Ana Vidaurre, José M Meseguer Dueñas, Isabel Castilla Cortázar (2008) Physical characterization of polycaprolactone scaffolds. *J Mater Sci Mater Med* 19: 189-195. [[Crossref](#)]
79. Ulises Gómez Pinedo, Leyre Sanchez Rojas, Sandra Vidueira, Francisco J Sancho, Cristina Martínez Ramos et al. Bridges of biomaterials promote nigrostriatal pathway regeneration. *J Biomed Mater Res B Appl Biomater* 107: 190-196. [[Crossref](#)]
80. Gopinathan Janarthanan, In Gul Kim, Eun Jae Chung, Insup Noh (2019) Comparative studies on thin polycaprolactone-tricalcium phosphate composite scaffolds and its interaction with mesenchymal stem cells. *Biomater Res* 23: 1. [[Crossref](#)]
81. Konstanty Szuldrzyński, Miłosz Jankowski, Daniel P Potaczek, Anetta Undas (2020) Plasma Fibrin Clot Properties as Determinants of Bleeding Time in Human Subjects: Association with Histidine-Rich Glycoprotein. *Dis Markers* 2020: 7190828. [[Crossref](#)]
82. Andrew L Frelinger 3rd, Anja J Gerrits, V Bogdan Neculaes, Thomas Gremmel, Andrew S Torres et al. (2018) Tunable activation of therapeutic platelet-rich plasma by pulse electric field. Differential effects on clot formation, growth factor release, and platelet morphology. *PLoS One* 13: e0203557. [[Crossref](#)]
83. Román F Jiménez Aristizabal, Catalina López, María E Álvarez, Carlos Giraldo, Marta Prades et al. (2017) Long-term cytokine and growth factor release from equine platelet-rich fibrin clots obtained with two different centrifugation protocols. *Cytokine* 97: 149-155. [[Crossref](#)]
84. Mihai Bucur, Carolina Constantin, Monica Neagu, Sabina Zurac, Octavian Dinca et al. (2019) Alveolar blood clots and platelet-rich fibrin induce in vitro fibroblast proliferation and migration. *Exp Ther Med* 17: 982-989. [[Crossref](#)]
85. Jan Gessmann, Dominik Seybold, Fahim Ayami, Elvira Peter, Hinnerk Baecker et al. (2018) Peripheral Blood Plasma Clot as a Local Antimicrobial Drug Delivery Matrix. *Tissue Eng Part A* 24: 809-818. [[Crossref](#)]
86. John W Weisel, Rustem I Litvinov (2013) Mechanisms of fibrin polymerization and clinical implications. *Blood* 121: 1712-1719. [[Crossref](#)]